

Effect of the Ion Mass and Energy on the Response of 70-nm SOI Transistors to the Ion Deposited Charge by Direct Ionization

Mélanie Raine, *Student Member, IEEE*, Marc Gaillardin, *Member, IEEE*, Jean-Etienne Sauvestre, *Member, IEEE*, Olivier Flament, *Senior Member, IEEE*, Arnaud Bournel, and Valérie Aubry-Fortuna

Abstract—The response of SOI transistors under heavy ion irradiation is analyzed using Geant4 and Synopsys Sentaurus device simulations. The ion mass and energy have a significant impact on the radial ionization profile of the ion deposited charge. For example, for an identical LET, the higher the ion energy per nucleon, the wider the radial ionization track. For a 70-nm SOI technology, the track radius of high energy ions (> 10 MeV/a) is larger than the transistor sensitive volume; part of the ion charge recombines in the highly doped source or drain regions and does not participate to the transistor electric response. At lower energy (< 10 MeV/a), as often used for ground testing, the track radius is smaller than the transistor sensitive volume, and the entire charge is used for the transistor response. The collected charge is then higher, corresponding to a worst-case response of the transistor. Implications for the hardness assurance of highly-scaled generations are discussed.

Index Terms—Bipolar gain, Geant4 and device simulations, heavy ion irradiation, radial ionization profile, SOI transistors.

I. INTRODUCTION

THE analysis of the transistor response to heavy ion irradiation is of particular importance to understand the Single-Event Effects (SEE) observed in integrated circuits used in space environment. The JEDEC standard [1] defining the procedures for SEE testing of integrated circuits clearly states that “the end product of the test is a plot of the SEE cross-section vs. effective Linear Energy Transfer (LET)”. The sensitivity of a circuit to SEE is thus only analyzed in terms of LET. The underlying hypothesis is that the device response is the same for ions with different energies but same LET. This assumption is the basis for SEE testing which uses low energy ions (usually in the 1–100 MeV/a energy range) to experimentally simulate the large spectrum of ion energy encountered in space (up to hundreds of GeV/a) [2], [3].

However previous work using low energy ions with different energies but same LET has shown that the energy has some impact on charge collection in CMOS/SOS (Silicon on Sapphire)

structures [4]. On the other hand, another study performed on $0.5 \mu\text{m}$ to $1 \mu\text{m}$ generation bulk devices demonstrated that the difference induced by the ion energy is not significant compared with other experimental uncertainties [5]. More generally, as the size of the transistor sensitive volume is decreased with the technology generation, the question of the applicability of LET as an appropriate metric to study the SEE has arisen ([6], [7] and references therein). Former work (e.g., [8], [9]) has studied the radial distribution of deposited charges around the ion path. Devices with small sensitive volume like SOI might be sensitive to this radial extension of the ion deposited charge, i.e., to the ion mass and energy. Experimental work on SOI devices reported in [10] has for example shown a lower collected charge for high energy ions compared to low energy ones with close LET.

Based on these considerations, the aim of this study is to analyze through simulation the response of a 70-nm gate length partially depleted (PD) SOI transistor [10] to irradiation with heavy ions at the same LET but different energy¹. In particular, we will show that differences in the transistor response may be observed at the same LET, contrary to underlying assumptions of the JEDEC standards.

The Geant4 simulation toolkit is used to simulate the radial ionization profile of ions with close LETs but different energies. Limits and validity of Geant4 track structures are discussed and compared with previously published results ([11], [12]). The radial ionization profiles are then used as inputs into Synopsys Sentaurus device simulations. It will be shown that the transistor response is significantly enhanced for the lowest energy ion. At first order, the transistor response is determined by the charge deposited in its sensitive volume.

II. DESCRIPTION OF SIMULATIONS

A. Geant4 Simulation

Monte Carlo Geant4 simulations are used to model the radial ionization profile of an ion deposited charge. Geant4 is a simulation toolkit employing object-oriented methods and coded in C++, which allows simulating the passage of particles through matter [13]. In this work, Geant4 version 9.2 is used to build the simulation.

The developed test application simulates a mono-energetic ion beam, normally incident in a box made of natural silicon,

¹In the rest of the paper, if not otherwise stated, “ion energy” is intended as “ion kinetic energy per unit mass”.

Manuscript received September 10, 2009; revised December 15, 2009; accepted April 06, 2010. Date of current version August 18, 2010.

M. Raine, M. Gaillardin, J.-E. Sauvestre, and O. Flament are with CEA, DAM, DIF, F-91297 Arpajon, France.

A. Bournel and V. Aubry-Fortuna are with the Institut d'Electronique Fondamentale, CNRS, Université Paris Sud (UMR 8622), F-91405 Orsay, France.

Color versions of one or more of the figures in this paper are available online at <http://ieeexplore.ieee.org>.

Digital Object Identifier 10.1109/TNS.2010.2048926

with a 2- μm thick SiO_2 overlayer – representative of the overlayers of the studied transistor. The box size is larger than the sensitive volume of the transistor. The impact of the incident ion on the box is always at the center of the upper SiO_2 face.

Only electromagnetic interactions are considered, the focus being on the radial deposition of energy by delta rays around the ion path. The main process is thus ionization, activated both for incident ions and secondary electrons, but the used list of physics processes also includes other electromagnetic interactions for secondary electrons, positrons and photons. The Livermore low energy package [14] is used; it simulates the production of delta rays with energies above 250 eV. Below this threshold, electrons that should have been produced are considered as a local energy deposit. Effects of this limitation of Geant4 on our calculations are discussed further.

Our purpose is to simulate the radial distribution of charge deposited by a single ion. However, in order to get sufficient statistics, the radial distribution of the deposited charge is calculated from the averaged tracks of 10^4 incident ions. Coulomb scattering is simulated for electrons only; it is voluntarily turned off for incident ions. This way, the averaged radial track density is representative of the charge deposited by the delta electrons only. If the ion scattering was turned on, lateral straggling would be observed, resulting in a larger track than for a single ion. Simulations with and without ion scattering were conducted to check that turning it off did not significantly impact the value of LET in the region of active silicon. The maximum fluctuation is about 0.1%, which is negligible.

The spatial distribution of energy deposition from incident ion and secondary particles is scored in a histogram, for deposits in the active silicon film ($T_{\text{Si}} = 150 \text{ nm}$) located after the 2- μm silica overlayer. For each step, Cartesian coordinates of the deposits are randomly selected on the line connecting the pre- and post-step points. The radial distance of this point to the ion path is then calculated and the corresponding histogram bin incremented. To calculate the radial track structure, the deposited energy E is converted to a density N of electron/hole pairs:

$$N = \frac{E}{I_0} \cdot \frac{1}{N_{\text{ion}}} \cdot \frac{1}{V} \quad (1)$$

with $I_0 = 3.6 \text{ eV}$ the average energy needed to create an electron/hole pair in silicon, N_{ion} the number of incident ions and V the volume in which this energy E is summed, meaning the “volume” of an histogram bin, in cm^3 :

$$V = \pi \cdot (r_2^2 - r_1^2) \cdot T_{\text{Si}}. \quad (2)$$

Using this method, a detailed description of the track core is performed, down to the Angstrom range. Geant4 is hardly realistic at this atomistic scale since it considers a homogeneous material without taking into account the silicon crystalline structure and atoms positions. The crystalline structure would be of particular importance for the lowest energy electrons. However, this fine calculation of the radial deposited charge was necessary to accurately describe the dense core (with high concentration of carriers) and, by integration, the total deposited charge. At

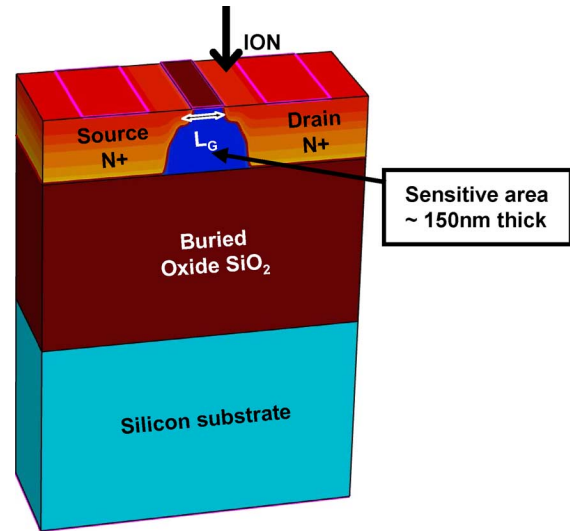


Fig. 1. Schematic representation of a partially depleted SOI transistor with gate length $L_G = 70 \text{ nm}$, extracted from Synopsys Sentaurus. The ion strikes the device in normal incidence at the body-drain junction (black arrow). The sensitive area (or body) appears in dark blue. The 2 μm SiO_2 overlayer is not depicted here.

the scale of the transistor (70 nm), the total charge deposited in the sensitive volume is relevant, even if the inner description of the track core is not.

B. Synopsys Sentaurus Device Simulation

The radial track structures obtained from Geant4 simulations, fitted with multiple Gaussians [15], are used as input data in the Synopsys Sentaurus device simulator [16]. The simulated struck device is a 3D-floating body SOI NMOS transistor (Fig. 1) biased in the OFF-state. This simulated device represents the 70 nm partially depleted SOI transistor tested in [10], for which the structure is known. The overlayers (omitted in Fig. 1) are made of 2 μm of silica; the active silicon film is 150-nm thick; the buried oxide thickness is 0.4 μm and the gate length is 70 nm.

Physical models activated in the simulation are: Schockley-Read-Hall (SRH) with doping-dependent lifetimes and Auger for carrier recombination and generation; bandgap narrowing model for intrinsic carrier concentration; doping-dependent model and transverse field dependence for mobility. The simple drift-diffusion model was selected.

The ion strikes the device in normal incidence at the body-drain junction, where the electric field is maximum, to simulate the transistor worst case response [17]–[19], i.e., the maximum drain collected charge and bipolar amplification (bipolar gain). The LET value is considered constant along the ion track in the 150-nm silicon film; the track structure is thus also kept constant. In order to analyze the transistor response, the simulated transient current recorded at the drain electrode is integrated to get the collected charge. The parasitic bipolar gain, which characterizes the transistor response, is then calculated by the ratio of the collected charge at the drain electrode to the deposited charge by the incident ion in the transistor silicon film. In our simulations, the value of the collected charge used to calculate the bipolar gain corresponds to the charge collected 1 ns after

the ion strike. The deposited charge is calculated by integration of the entire radial charge profile in the silicon film (assuming infinite lateral dimensions). The deposited charge is then proportional to the ion LET and to the thickness of the silicon film. All deposited charge and LET values used in this paper are calculated from Geant4 simulations.

III. SIMULATIONS OF THREE IONS WITH CLOSE LET AND DIFFERENT ENERGY

A. Geant4 Radial Track Structures

Three ions are simulated with Geant4, chosen with close LET and different energies:

- ^{48}Ca , 2 MeV/a, LET = 21.7 MeV · cm²/mg.
- ^{78}Kr , 15 MeV/a, LET = 23.1 MeV · cm²/mg.
- ^{136}Xe , 45.5 MeV/a, LET = 23.5 MeV · cm²/mg.

The radial track structures, i.e., the density of deposited charge versus the track radius, obtained for the three ions are plotted in Fig. 2(a). They are compared to the corrected Katz analytical track model described by Waligorski in [20] and adapted to silicon by Fageeha in [11], in dashed lines in Fig. 2(a). Fig. 2(b) displays the cumulated deposited charge in the 150-nm silicon film obtained by integration of Fig. 2(a) curves.

In the micrometer range (radially from the ion path), the track radius of the high energy ion in Fig. 2(a) is larger than the low energy ion one. This is a well-known and expected result, consistent with previous studies ([5], [21]) and Fageeha's analytical tracks [11]. Geant4 and Fageeha's tracks fit well above 10–20 nm.

However, in the nanometer range, significant differences between the two models appear, the three Fageeha's tracks being practically identical, while the Geant4 tracks differ from one to another and from Fageeha's. Calculations based on Kobetich and Katz theory [8] like Fageeha's are known to be inappropriate for the track core region [12], because they do not correctly treat the transport of low energy electrons. With the production threshold of 250 eV for delta electrons previously mentioned, Geant4 could be pointed out to have the same limitation. However, integrating Geant4 radial profiles gives much closer LETs as calculated by SRIM than Fageeha's profiles (Table I).

The Geant4 and SRIM values are very close for the lighter ion (calcium). For heavier ions (krypton and xenon), Geant4 tends to slightly underestimate the LET value compared to SRIM, with a maximum variation of 15% for xenon. It must be noted that recent measurements performed at Jyväskylä facility shows that SRIM overestimates the LET of heavy ions (krypton and xenon), by 10% at maximum for xenon [22]. Unfortunately, these measurements were only made at energies up to ~ 9 MeV/a; no experimental values are thus available to compare with the 15 MeV/a krypton and the 45.5 MeV/a xenon. Considering these uncertainties on the LET values in SRIM, the Geant4 calculation is considered as a good estimate of the real LET.

Recent work by Murat [12], considering the electron energies down to 1.5 eV, does not have the same inadequacies for the transport of low energy electrons. It provides much more accurate track structures, particularly in the track core. However,

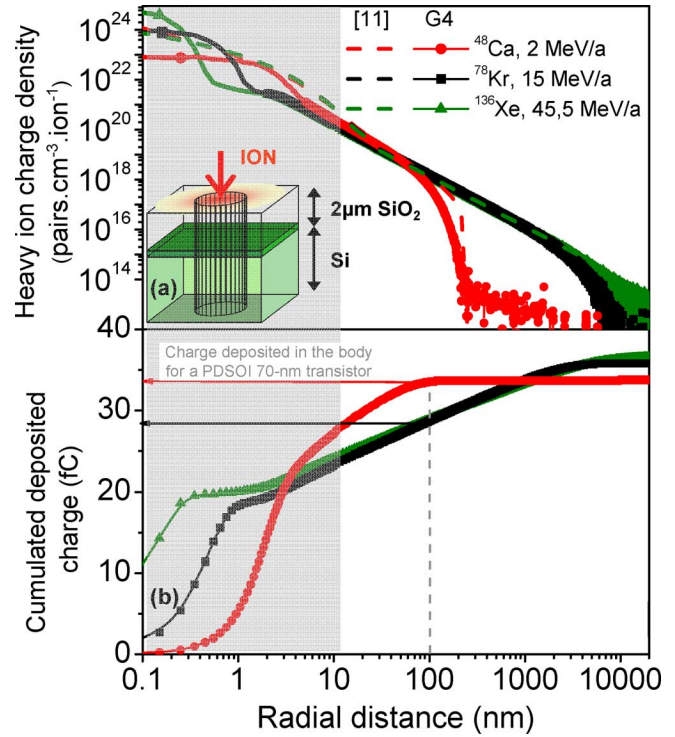


Fig. 2. Geant4 simulations of (a) the radial pair density profile and (b) the cumulated deposited charge as a function of radial distance for low energy (2 MeV/a ^{48}Ca , LET ~ 22 MeV · cm²/mg), medium energy (15 MeV/a ^{78}Kr , LET ~ 23 MeV · cm²/mg) and high energy ions (45.5 MeV/a ^{136}Xe , LET ~ 23 MeV · cm²/mg). The ions are normally incident in a silicon box with 2 μm of SiO₂ overlayer (see inset in Fig. 2(a)). The deposited energy is recorded in a 150-nm silicon film below the 2 μm silica overlayer. In Fig. 2(a), Geant4 tracks are represented along with analytical calculations performed with Fageeha's model [11] (dashed lines). In the grey tint part, all three dashed lines are superimposed. In Fig. 2(b), arrows illustrate the deposited charge in a 70-nm SOI transistor's sensitive area. The grey tint part corresponds to the range where Geant4 physics is debatable.

TABLE I
CALCULATIONS OF LET IN THE TRANSISTOR SENSITIVE VOLUME FOR THE THREE STUDIED IONS, WITH SRIM AND BY INTEGRATION OF FAGEEHA'S AND GEANT4 TRACK STRUCTURES.

Ion	Energy [MeV/a]	LET [MeV.cm ² /mg]		
		SRIM	Fageeha	Geant4
^{48}Ca	2	21.6	30.1	21.7
^{78}Kr	15	25.9	36.6	23.1
^{136}Xe	45.5	27.5	36.7	23.5

[12] focuses on protons while our interest here is on heavy ions. Moreover, Geant4 is a widely used and accessible tool; it is thus interesting to use it to simulate track structures, and particularly to discuss its limitations. Underlying physics for delta electrons emission and transport is thus briefly analyzed, to quantify in what extent Geant4 tracks are reliable.

The emission of delta electrons by an incident ion of total kinetic energy T_{ion} and mass M is ruled by elastic scattering kinematics. This results in a simple relation ((3)) between the energy T_{e^-} transferred to delta electrons (mass m) by the incident ion and their angle of emission from the ion path θ :

$$T_{e^-} = \frac{4Mm}{(M+m)^2} T_{\text{ion}} \cos^2 \theta. \quad (3)$$

First, according to this formula, the transferred energy has an upper limit T_{\max} (for $\theta = 0$) directly linked to the ion energy. So, the higher the ion energy, the higher the maximum energy of its delta electrons and the larger their range. This is the reason for the increase of the track radius with the ion energy previously mentioned.

Second, relation (3) shows that very low energy electrons – which are not produced for energies below 250 eV – should be emitted orthogonally to the ion path. In a complete model, these 250 eV electrons would have had generated other electrons, within a range of several nm (2 nm in [12], 5 nm in [23]). Instead, the electron energy is locally deposited without taking into account the motion of electrons. This explains the very high density observed in the track core in Fig. 2(a). The region where the track core is known to be poorly described can be limited to the nanometer range (below 10 nm, grey part in Fig. 2).

Apart from the track core, secondary delta electrons are emitted by first generation ones, also with an angular distribution. This produces a cloud of electrons travelling with erratic trajectories. At large radius values, the range of 250 eV electrons appears very small compared to the range on which the track structures vary (both axes in Fig. 2(a) are plotted on a log scale). On average, local deposits of energy thus seem a good approximation for this part of the curve. Comparison with the Fageeha's model [11] confirms that above 10 nm, the radial profile becomes realistic.

Since integration of Geant4 tracks provides a reliable value for LET (Table I), the deposited charge at the transistor scale (70 nm) can be considered as relevant, even if the inner description of the track core is not. In the next section, device simulations will show that this description is good enough for our study.

B. *Sentaurus* Synopsys Simulation Results

Device simulations are then performed with Synopsys Sentaurus using Geant4 radial track structures as inputs. The aim is to simulate qualitative trends for a 70-nm PDSOI transistor irradiated with different ions, using realistic track structures – instead of Gaussian track structures often used in device simulations. In order to minimize the errors in deposited charge, much attention is paid to the Gaussian fits of Geant4 tracks and to the meshing of the structure in Synopsys Sentaurus, which is adapted to the track resolution. For all the bipolar gain calculated here, the error bar introduced is between -2% and $+3\%$.

1) *Validation of the Simulation Flow: Comparison With Experiments:* In order to gain confidence in the simulation results, calculations are first performed to compare simulations with experimental results presented in [10] for three partially depleted SOI technologies: 0.25 μm , 0.13 μm and 70 nm. Results for 6.2 MeV/a ^{48}Ca ion are reported in Fig. 3 (blue stars), along with corresponding experimental results extracted from [10]. For all three technologies, the simulated gain vs. collected charge exhibits a good agreement with experimental observations.

For the 70-nm technology, several simulated parasitic bipolar gains are reported. They correspond to different ion strike locations in the device (only one strike location is reported for the two other technologies). Fig. 4 illustrates the response of

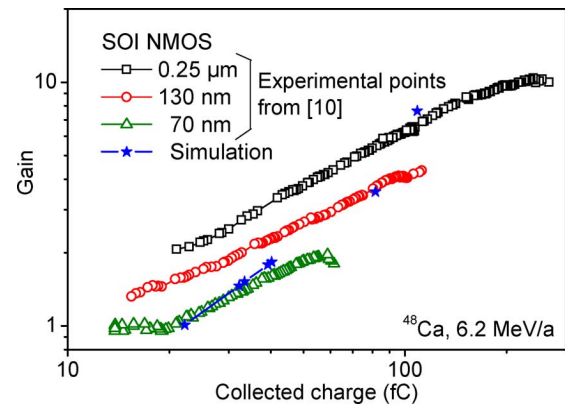


Fig. 3. Bipolar gain in 0.25- μm , 130-nm and 70-nm gate length partially depleted SOI transistors: experimental measurements for irradiation at GANIL with 6.2 MeV/a ^{48}Ca (open symbols), and simulation results (blue stars).

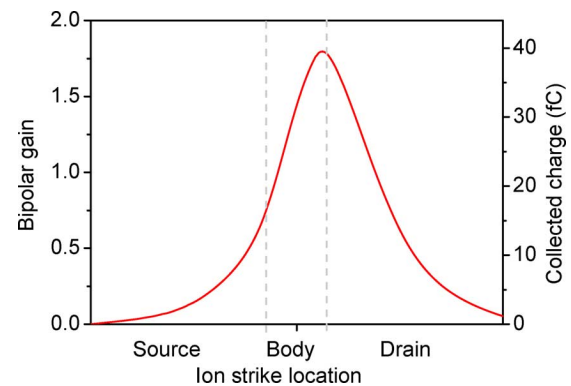


Fig. 4. Simulation results for a 6.2 MeV/a ^{48}Ca ion in a 70-nm PDSOI transistor: bipolar gain and collected charge as a function of the ion strike location.

the transistor as a function of the ion strike location. It confirms that an ion strike at the body-drain junction gives the transistor worst-case response, i.e., the most efficient bipolar amplification. For any other location, the collected charge and thus the bipolar gain are simply lower. Experimental results also exhibit a larger range of collected charge than the simulated one. Simulation indeed represents an ideal case where the deposited charge is always the same and corresponds to the average experimental deposited charge.

All calculated values fit well the experimental statistic presented in [10], giving good confidence both in the ion radial ionization profile calculated with Geant4 and used in Synopsys Sentaurus and in the simulated 3D device structure.

Other simulations were performed with various energies for different ions, giving similar results. These simulations are not more extensively presented here to keep the analysis focused on our main subject: the response of a given SOI transistor to irradiation with heavy ions at the same LET but different energy.

2) *Effect of the Ion Mass and Energy on the 70-nm Device Transient Response:* Drain transient currents and collected charges extracted from simulations are displayed in Fig. 5, for the three ions presented in Fig. 2. The general shape of transient currents is similar for the three ions but the amplitude of peak current and transient width vary.

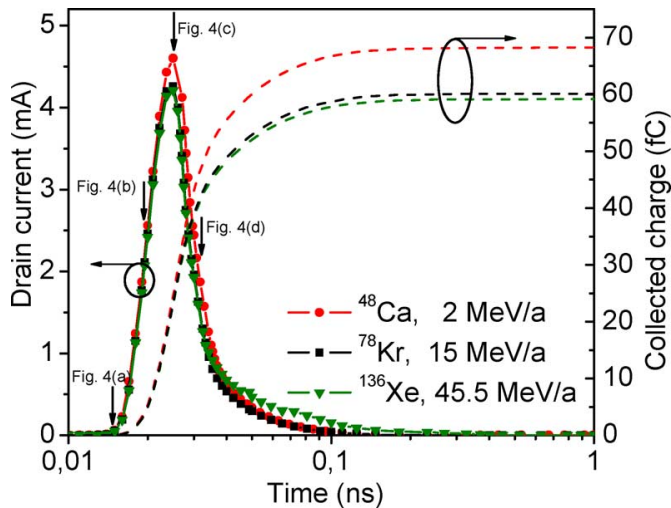


Fig. 5. Device simulation results for low energy (^{48}Ca , 2 MeV/a), medium energy (^{78}Kr , 15 MeV/a) and high energy (^{136}Xe , 45.5 MeV/a) normally incident ions in a 70-nm partially depleted SOI transistor: drain current transient (symbols) and collected charge (dashed lines). Arrows are related to instants used in Fig. 6(a)–(d).

Calculated gains for 70-nm SOI transistors are reported in Table II. Both medium and high energy ions have similar bipolar gain, while the gain of the lower energy ion is about 25% higher. This trend is the same as experimentally observed in [10]: the maximum bipolar gain is lower for a high energy ion compared to a low energy ion having close LET.

To analyze the impact of geometrical factors on the transistor response, we must first consider the size of the transistor, and more specifically of its sensitive volume (i.e., the body region, in dark blue in Fig. 1), compared to the track radius. Please remember here that the deposited charge – similar for the three ions – is calculated in a silicon film with infinite lateral dimensions. The radial extension of the track (corresponding to a drop of the density in Fig. 2(a) and a saturation of the cumulated deposited charge in Fig. 2(b)) is of about 200 nm for calcium, 6 μm for krypton and more than 20 μm for xenon. However, the injected charges will trigger the transistor mainly when their density exceeds the doping concentration in the device, i.e., in the body. The three ion tracks are thus larger than the transistor's sensitive volume (see arrows in Fig. 2(b)). As a consequence, the actual charge deposited in the body is different for the three ions. The values extracted from the simulation are reported in Table II, as percentages of the total deposited charge. Krypton and xenon deposit similar amount of charge, while calcium deposits 25% more charge (Table II). This is close to the difference observed in bipolar gain – calculated as the ratio of the collected charge to the *total* deposited charge. The difference in transistor response can thus be explained by geometrical factors – less charge actually deposited in the sensitive volume, lower bipolar gain.

Therefore, the important parameter is the *amount* of charge deposited in the sensitive volume, no matter *how* this charge is deposited. In other words, the track structure in the sensitive volume does not seem to matter for charge collection, as long as the integral of this track is kept constant. This feeling is reinforced by the examination of cross-sections of electron density

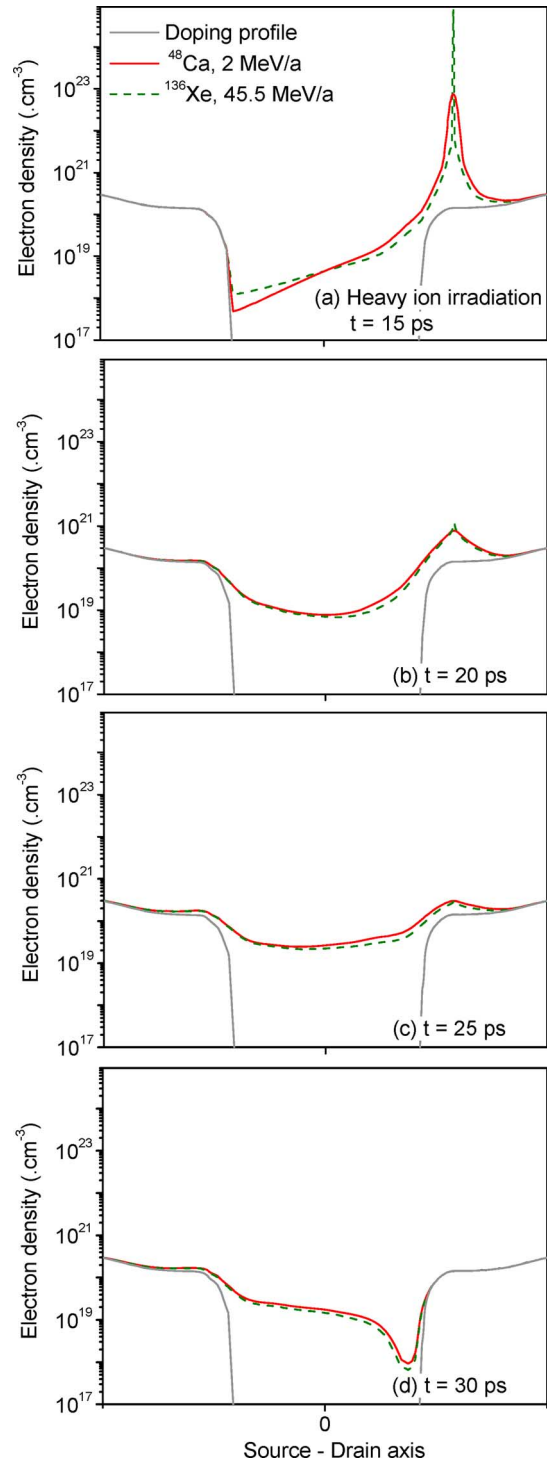


Fig. 6. Cross-sections of the electron density in the sensitive volume of the 70-nm PDSOI transistor, at different instants of the simulation, for ^{48}Ca , 2 MeV/a and ^{136}Xe , 45.5 MeV/a. In grey, the electron density in the device before the ion cross, corresponding to the doping profile.

in the body at different instants of the simulation, represented in Fig. 6(a)–(d) for calcium and xenon (krypton was omitted for the sake of clarity, curves being very close to those of xenon). Corresponding instants on the current transients are represented with arrows in Fig. 5. While the injected track structures are very different (Fig. 6(a), corresponding to Fig. 2(a)), particularly in the track core (log scale), these differences are quickly

TABLE II
SIMULATED VALUES OF BIPOLAR GAIN AND PERCENTAGE OF CHARGE DEPOSITED IN THE SENSITIVE VOLUME OF THE 70-nm SOI TRANSISTOR (I.E., THE BODY REGION) FOR THREE DIFFERENT IONS WITH CLOSE LET. PERCENTAGE OF AVAILABLE CHARGE IN THE BODY AFTER 20 ps

Ion	Energy [MeV/a]	LET [MeV.cm ² /mg]	Simulated bipolar gain	% of deposited charge in the body	% of available charge after 20 ps
⁴⁸ Ca	2	21.7	2.0	99%	37%
⁷⁸ Kr	15	23.1	1.7	81%	30%
¹³⁶ Xe	45.5	23.5	1.6	79%	30%

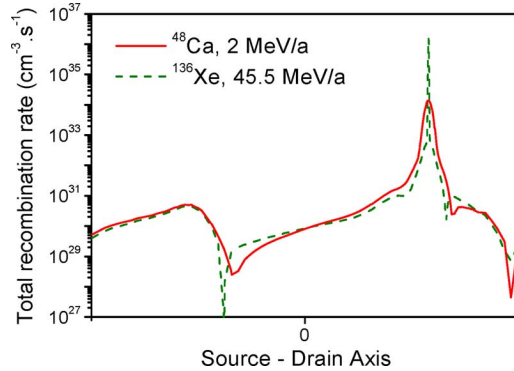


Fig. 7. Cross-sections of the total recombination rate in the sensitive volume of the 70-nm PDSOI transistor, just after the injection of charge by the incident ion, for ⁴⁸Ca, 2 MeV/a and ¹³⁶Xe, 45.5 MeV/a.

softened by the transistor behavior. At 20 ps (Fig. 6(b)), just after irradiation, differences in the track core structure almost disappear. This is due to the diffusion of charges, but also to a strong initial recombination, particularly important in the track core just after the injection of charge by the incident ion (Fig. 7). The charge available in the body is calculated by integration of the total excess charge, which may be observed in Fig. 6 as the difference between colored curves and the grey one. This last curve represents the electron density in the device before the ion cross, corresponding to the doping profile. Just after the ion cross (at 20 ps, Fig. 6(b)), this available charge is smaller than what was initially deposited (at 15 ps, Fig. 6(a), see values in Table II). Then, this charge density increases again (Fig. 6(c)), maximum amplitude of current in Fig. 5) – which corresponds to the bipolar amplification – while the recombination rate decreases.

After this important initial recombination, the same amount of charge is available in the body for krypton and xenon, while 23% more charge is available in the case of calcium (Fig. 6(b)). So, even if the differences in track cores are rapidly softened, the difference in charge available for collection stays the same and is similar to the final difference of 25% in bipolar gain.

IV. SENSITIVITY OF 70 NM PDSOI TRANSISTOR TO DIFFERENT HEAVY IONS AND ENERGIES

Additional simulations are performed, to study the ionizing effects of ions with different masses and energies. Fig. 8 shows the calculated gain as a function of LET for four ions: nitrogen, calcium, krypton and xenon. The minimum energy simulated here for each ion corresponds to the energy giving the maximum

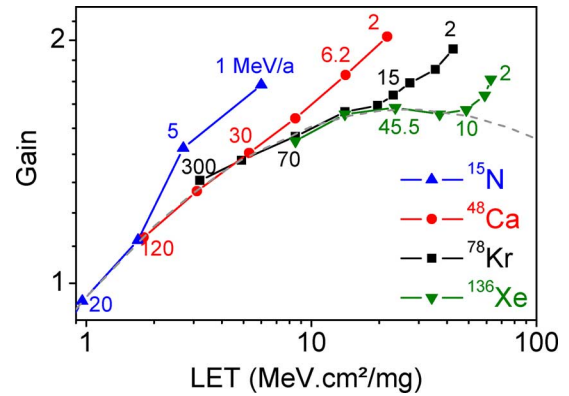


Fig. 8. Calculated bipolar gain as a function of LET (log-log scale) for four ions with different mass (nitrogen, calcium, krypton and xenon). The LET varies with the ion energy. The numbers close to the curve points correspond to the ion energy in MeV/a. Only few values are represented to give some references while keeping the figure as clear as possible. The grey dashed line corresponds to a common trend from which each ion deviates below a threshold energy.

LET for a normally incident ion. It is clear in Fig. 8 that the bipolar gain is not only a function of the LET but also of the ion mass and energy.

First, for a given ion, the bipolar gain increases with increasing LET and decreasing energy. This trend can be explained by the same kind of argument as previously used, i.e., the higher the ion energy, the wider the radial ionization profile. Thus, a more important proportion of charge being deposited in the body for a lower energy ion (see Table II), the bipolar gain increases with decreasing energy.

Second, it seems that the gain versus LET curves follow the same trend for every ion at high energy (grey dashed line in Fig. 8, linking $\log(\text{Gain})$ to $\log(\text{LET})$ with a quadratic). This trend looks like classical variations of the bipolar gain with the collector current ([18], [24], [25]), which are explained as follows.

For low values of LET, corresponding to low-injection conditions, the parasitic bipolar transistor is only partly triggered; the concentration of carriers generated during irradiation is not high enough to completely forward bias the body-source junction. The bipolar gain is thus low and increases with LET, i.e., with the increase in carrier concentration.

For intermediate values of LET, the bipolar gain is maximal. For the technology of concern, this corresponds to an LET around 20 MeV · cm²/mg, which is relatively high. This is due to the quite high body doping, inherent to the short gate length of this PD SOI transistor.

For high values of LET, corresponding to high-injection conditions, there is a saturation of the parasitic bipolar transistor response. Recombination processes are now dominant, leading to a decrease in bipolar gain. This is a common behavior for all SOI technology generations. This part is only initiated here with xenon.

The particular behavior observed in this study is the deviation at low energy. In Fig. 8, for a given ion, when the energy decreases below a certain threshold, the ion curve deviates from the common trend. Applying again the same kind of argument as in the previous paragraph, it appears that for every point on the dashed grey line in Fig. 8, the same proportion of charge is

deposited in the transistor's body (around 80% of the total deposited charge). So, the deviation at low energy corresponds for every ion to an increase in the proportion of charge deposited in the body and available after initial recombination.

In the end, the explanation for the difference in bipolar gain between two particular ions with the same LET presented in the previous paragraph can be generalized to all ions and LET. For different ions with the same LET, the bipolar gain will thus be the same if the same proportion of the total charge is deposited in the body, and different if not. The difference will be more or less important depending on the proportion of charge deposited in the body and on the available charge after initial recombination. All is thus dependent on the track structures, with a more or less large track, compared to the transistor's sensitive volume dimensions.

V. DISCUSSION

Differences in bipolar gain calculated here are quite small, with a maximum difference of 25% between gains of 1.6 and 2.0. Still, those effects could be significant at the integrated circuit level. Indeed, these differences are related to a more or less important floating body effects. These effects have been shown to be relevant for SET pulse broadening in SOI inverter chains [26], [27]. It is thus possible that quite small differences like those observed here lead to much more important effects in an inverter chain. Additional simulations would be necessary to confirm or invalidate this hypothesis.

This work was performed for a given transistor structure, in a given generation. Differences being linked to the size of the sensitive volume, it seems that results will be similar for all transistors in a given technology generation, as long as changes in geometry do not lead to different active volumes. However, it is quite difficult to draw trends for more integrated transistors, mainly because of the limitations encountered in track simulations. Indeed we showed that the track structure is not important *inside* the sensitive volume. In our case, this volume is still big enough to allow the use of Geant4 tracks. An evaluation from Fig. 2(a) shows that these tracks may be used for technology generation as integrated as the 45 nm generation. However, to study more integrated technologies, a more accurate description of the track core is needed, which is not possible with the current Geant4 production threshold for secondary electrons. Improvements of the model are thus needed to take into account lower energy electrons, as available in Murat's approach [12]. The DNA project of the Geant4 community [28] seems promising, providing the actual model, restricted to liquid water, is generalized to other materials (silicon in particular).

An important particularity of our study is obviously the small volume inherent to SOI structures. It would also be interesting to get insights into the response of bulk transistors. However, such transistors involve complex doping profiles [29], to which track structures need to be compared. A complete study is thus needed and no trends may be driven from the present one.

Usual facilities used for SEE testing deliver ion beams with energies in the order of a few MeV/a. For the particular technology studied here, at a given LET, the collected charge is maximized for a lower energy ion. According to these results

(Fig. 8), test cases may thus be considered conservative. However, these small energies may lead to other issues. We can take the example of xenon at 3.5 MeV/a, a commonly used ion to test CMOS devices [30]. In a standard device, this ion has to go through 10 to 12 μm of silica and metal – which are common overlayers for 65 and 45 nm generation devices – before reaching active silicon. After these overlayers, its energy is only around 2 MeV/a. The deposited and thus collected charge is then overestimated, compared to another ion with same “incident LET” but with higher energy, whose energy only varies a little in overlayers. Testing with low energy ions to represent high energy ions with same LET may thus lead to erroneous results (the tested LET is indeed different). However, as seen previously, these tests are in fact conservative – as soon as only direct ionization effects are taken into account. Indeed, previous studies have also found differences in SEE sensitivity due to secondary ionization [7], [31] – this time mainly for high energy ions.

Another underlying limit that we must be aware of for testing is the accounting for a fixed value of LET for a given ion and energy. This value is actually a mean value. Indeed, the straggling induced by ion scattering can lead to a distribution in LET, i.e., in deposited charge [32], [33], particularly if a low energy incident ion has to go through thick overlayers before reaching the sensitive volume. Moreover, using an average track structure as done in this work supposes a cylindrical symmetry of energy deposition. However, a single ion may have an asymmetric radial dose profile [33]. These excursions outside of the average ion track may induce variations in collected charge and thus give a distribution on the transistor response.

Finally, one should bear in mind when referring to an LET value that this value is highly dependent on the software used to calculate it (Table I, [22], [34]), particularly for very heavy ions like krypton or xenon. This uncertainty should be considered when analyzing variations in transistor response, especially when these variations are close to the uncertainties in the stopping power ($\sim 10\%$).

VI. CONCLUSION

In this work, Geant4 simulations of the radial ionization tracks of heavy ions in silicon, along with device simulations, are performed to analyze the response of a 70-nm SOI transistor under heavy ion irradiation. Simulation results show that the LET is not the only parameter to characterize the transistor response. The incident ion mass and energy, determining the track structure, must also be considered. The track radius of high energy ions (> 10 MeV/a) is indeed larger than the transistor sensitive volume; part of the ion charge recombines in the highly doped source or drain regions and does not participate to the transistor electric response. At lower energy (< 10 MeV/a), often used for ground testing, the track radius is smaller than the transistor sensitive volume, and the entire charge is used for the transistor response. The collected charge is then higher, corresponding to a worst-case response of the transistor. Consequently, SEE testing using low energy ions to experimentally simulate the large spectrum of ion energy encountered in space may be considered conservative.

ACKNOWLEDGMENT

The authors would like to thank V. Ferlet-Cavrois from ESA/ESTEC for her contribution and the useful discussions we had on this work.

REFERENCES

- [1] EIA/JESD57: Test Procedure for the Measurement of Single-Event Effects in Semiconductor Devices From Heavy Ion Irradiation 1996.
- [2] J. L. Barth, "Modeling space radiation environments," in *Nuclear and Space Radiation Effects Conference Short Course*, Snowmass, CO, 1997.
- [3] P. E. Dodd, J. R. Schwank, M. R. Shaneyfelt, V. Ferlet-Cavrois, P. Paillet, J. Baggio, G. L. Hash, J. A. Felix, K. Hirose, and H. Saito, "Heavy ion energy effects in CMOS SRAMs," *IEEE Trans. Nucl. Sci.*, vol. 54, pp. 889–893, Aug. 2007.
- [4] W. J. Stapor, P. T. McDonald, A. R. Knudson, A. B. Campbell, and B. G. Glagola, "Charge collection in silicon for ions of different energy but same linear energy transfer (LET)," *IEEE Trans. Nucl. Sci.*, vol. 35, pp. 1585–1590, Dec. 1988.
- [5] P. E. Dodd, O. Musseau, M. R. Shaneyfelt, F. W. Sexton, C. D'hose, G. L. Hash, M. Martinez, R. A. Loemker, J.-L. Leray, and P. S. Winokur, "Impact of ion energy on single-event upset," *IEEE Trans. Nucl. Sci.*, vol. 45, pp. 2483–2491, Dec. 1998.
- [6] M. A. Xapsos, "Applicability of LET to single events in microelectronic structures," *IEEE Trans. Nucl. Sci.*, vol. 39, pp. 1613–1621, Dec. 1992.
- [7] R. A. Reed, R. A. Weller, M. H. Mendenhall, J.-M. Lauenstein, K. M. Warren, J. A. Pellish, R. D. Schrimpf, B. D. Sierawski, L. W. Massengill, P. E. Dodd, M. R. Shaneyfelt, J. A. Felix, J. R. Schwank, N. F. Haddad, R. K. Lawrence, J. H. Bowman, and R. Conde, "Impact of ion energy and species on single event effects analysis," *IEEE Trans. Nucl. Sci.*, vol. 54, pp. 2312–2321, Dec. 2007.
- [8] E. J. Kobetich and R. Katz, "Energy deposition by electron beams and delta rays," *Phys. Rev.*, vol. 170, pp. 391–396, Jun. 1968.
- [9] A. Akkerman and J. Barak, "Ion-track structure and its effects in small size volumes of silicon," *IEEE Trans. Nucl. Sci.*, vol. 49, pp. 3022–3031, Dec. 2002.
- [10] V. Ferlet-Cavrois, P. Paillet, M. Gaillardin, D. Lambert, J. Baggio, J. R. Schwank, G. Vizkelethy, M. R. Shaneyfelt, K. Hirose, E. W. Blackmore, O. Faynot, C. Jahan, and L. Tosti, "Statistical analysis of the charge collected in SOI and bulk devices under heavy ion and proton irradiation – Implications for digital SETs," *IEEE Trans. Nucl. Sci.*, vol. 53, pp. 3242–3252, Dec. 2006.
- [11] O. Fageeha, J. Howard, and R. C. Block, "Distribution of radial energy deposition around the track of energetic particles in silicon," *J. Appl. Phys.*, vol. 75, 1994.
- [12] M. Murat, A. Akkerman, and J. Barak, "Electron and ion tracks in silicon: Spatial and temporal evolution," *IEEE Trans. Nucl. Sci.*, vol. 55, pp. 3046–3054, 2008.
- [13] S. Agostinelli *et al.*, "GEANT4 – A simulation toolkit," *Nucl. Instr. and Meth. in Phys. Res. A*, vol. 506, pp. 250–303, Jul. 2003.
- [14] S. Chauvie, S. Guatelli, V. Ivanchenko, F. Longo, A. Mantero, B. Mascialino, P. Nieminen, L. Pandola, S. Parlati, L. Peralta, M. G. Pia, M. Piergentili, P. Rodrigues, S. Saliceti, and A. Trindade, "Geant4 Low energy electromagnetic physics," in *IEEE Nucl. Sci. Symposium Conference Record*, Oct. 2004.
- [15] T. Makino, D. Kobayashi, K. Hirose, Y. Yanagawa, H. Saito, H. Ikeda, D. Takahashi, S. Ishii, M. Kusano, S. Onoda, T. Hirao, and T. Ohshima, "LET Dependence of single event transient pulse-widths in SOI logic cell," *IEEE Trans. Nucl. Sci.*, vol. 56, pp. 202–207, Feb. 2009.
- [16] Sentaurus Device Manual, Release v.2008.09 ed. Synopsys, 2008.
- [17] P. E. Dodd, M. R. Shaneyfelt, K. M. Horn, D. S. Walsh, G. L. Hash, T. A. Hill, B. L. Draper, J. R. Schwank, F. W. Sexton, and P. S. Winokur, "SEU-Sensitive volumes in bulk and SOI SRAMs from first-principles calculations and experiments," *IEEE Trans. Nucl. Sci.*, vol. 48, pp. 1893–1903, Dec. 2001.
- [18] V. Ferlet-Cavrois, G. Gasiot, C. Marcandella, C. D'Hose, O. Flament, O. Faynot, J. d. P. d. Pontcharra, and C. Raynaud, "Insights on the transient response of fully and partially depleted SOI technologies under heavy-ion and dose-rate irradiations," *IEEE Trans. Nucl. Sci.*, vol. 49, pp. 2948–2956, Dec. 2002.
- [19] T. Colladant, O. Flament, A. L'Hoir, V. Ferlet-Cavrois, C. D'Hose, and J. du Port de Pontcharra, "Study of transient current induced by heavy-ion in NMOS/SOI transistors," *IEEE Trans. Nucl. Sci.*, vol. 49, pp. 2957–2954, 2002.
- [20] M. P. R. Waligorski, R. N. Hamm, and R. Katz, "The radial distribution of dose around the path of a heavy ion in liquid water," *Nuclear Tracks and Radiation Measurement*, vol. 11, pp. 309–319, 1986.
- [21] O. Musseau, V. Ferlet-Cavrois, A. B. Campbell, A. R. Knudson, S. Buchner, B. Fischer, and M. Schlögl, "Technique to measure an ion track profile," *IEEE Trans. Nucl. Sci.*, vol. 45, pp. 2563–2570, 1998.
- [22] A. Javanainen *et al.*, "Linear energy transfer of heavy ions in silicon," *IEEE Trans. Nucl. Sci.*, vol. 54, pp. 1158–1162, 2007.
- [23] O. Kurniawan and V. K. S. Ong, "Investigation of range-energy relationships for low-energy electron beams in silicon and gallium nitride," *Scanning*, vol. 29, pp. 280–286, 2007.
- [24] S. M. Sze, *Physics of Semiconductor Devices*, Second ed. New York: Wiley, 1981, ch. 3.
- [25] V. Ferlet-Cavrois, C. Marcandella, G. Giraud, G. Gasiot, T. Colladant, O. Musseau, C. Fenouillet, and J. Du Port de Pontcharra, "Characterisation of the parasitic bipolar amplification in SOI technologies submitted to transient irradiation," *IEEE Trans. Nucl. Sci.*, vol. 49, pp. 1456–1461, 2002.
- [26] V. Ferlet-Cavrois *et al.*, "Investigation of the propagation induced pulse broadening (PIPB) effect on single event transients in SOI and bulk inverter chains," *IEEE Trans. Nucl. Sci.*, vol. 55, pp. 2842–2853, 2008.
- [27] P. Gouker *et al.*, "Generation and propagation of single event transients in 0.18- μm fully depleted SOI," *IEEE Trans. Nucl. Sci.*, vol. 55, pp. 2854–2860, 2008.
- [28] S. Chauvie *et al.*, "Geant4 Physics processes for microdosimetry simulation: Design foundation and implementation of the first set of models," *IEEE Trans. Nucl. Sci.*, vol. 54, pp. 2619–2628, 2007.
- [29] G. Gasiot, D. Giot, and P. Roche, "Alpha-induced multiple cell upsets in standard and radiation hardened SRAMs manufactures in a 65 nm CMOS technology," *IEEE Trans. Nucl. Sci.*, vol. 53, pp. 3479–3486, 2006.
- [30] G. Berger, "Experimental tools to simulate radiation environments/radiation effects," in *RADECS Short Course*, Bruges, 2009.
- [31] P. E. Dodd *et al.*, "Impact of heavy ion energy and nuclear interactions on single-event upset and latchup in integrated circuits," *IEEE Trans. Nucl. Sci.*, vol. 54, pp. 2303–2311, 2007.
- [32] R. A. Weller, A. L. Sternberg, L. W. Massengill, R. D. Schrimpf, and D. M. Fleetwood, "Evaluating average and atypical response in radiation effects simulations," *IEEE Trans. Nucl. Sci.*, vol. 50, pp. 2265–2271, 2003.
- [33] J. Barak and A. Akkerman, "Straggling and extreme cases in the energy deposition by ions in submicron silicon volumes," *IEEE Trans. Nucl. Sci.*, vol. 52, pp. 2175–2181, 2005.
- [34] A. Javanainen *et al.*, "Experimental linear energy transfer for heavy ions in silicon for RADEF cocktail species," *IEEE Trans. Nucl. Sci.*, vol. 56, pp. 2242–2246, 2009.